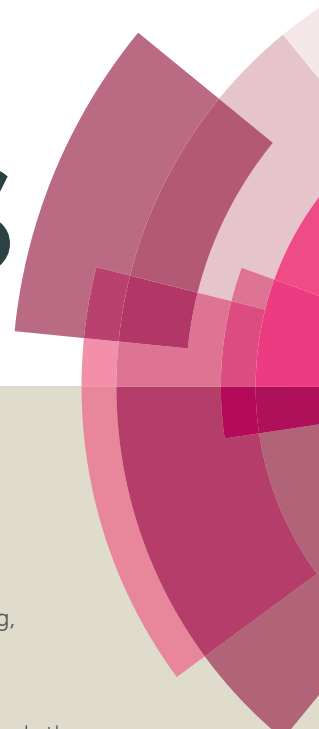


RSC Advances



This article can be cited before page numbers have been issued, to do this please use: L. Yang, D. Yang, Y. Chen, Q. Luo, M. Zhang, Y. Huang, Z. Lu, H. Sasabe and J. Kido, *RSC Adv.*, 2015, DOI: 10.1039/C5RA24186C.



This is an *Accepted Manuscript*, which has been through the Royal Society of Chemistry peer review process and has been accepted for publication.

Accepted Manuscripts are published online shortly after acceptance, before technical editing, formatting and proof reading. Using this free service, authors can make their results available to the community, in citable form, before we publish the edited article. This *Accepted Manuscript* will be replaced by the edited, formatted and paginated article as soon as this is available.

You can find more information about *Accepted Manuscripts* in the [Information for Authors](#).

Please note that technical editing may introduce minor changes to the text and/or graphics, which may alter content. The journal's standard [Terms & Conditions](#) and the [Ethical guidelines](#) still apply. In no event shall the Royal Society of Chemistry be held responsible for any errors or omissions in this *Accepted Manuscript* or any consequences arising from the use of any information it contains.

**Unsymmetrical squaraines with new linked manner for
high-performance solution-processed small-molecule organic
photovoltaic cells†**

Lin Yang,^{‡a} Daobin Yang,^{‡a,b} Yao Chen,^a Qian Luo,^a Mangang Zhang,^a Yan Huang,^{*a}
Zhiyun Lu,^{*a} Hisahiro Sasabe,^{*b} and Junji Kido^b

^a *Key Laboratory of Green Chemistry and Technology (Ministry of Education),
College of Chemistry, Sichuan University, Chengdu 610064, P. R. China. E-mail:
huangyan@scu.edu.cn, luzhiyun@scu.edu.cn*

^b *Department of Organic Device Engineering, Yamagata University, 4-3-16 Jonan,
Yonezawa, Yamagata 992-8510, Japan. Email: h-sasabe@yz.yamagata-u.ac.jp.*

[‡] The first two authors contributed equally to this work.

Abstract

Squaraines have been promising donor materials because of their strong and broad absorption band in the visible and near infrared regions which is suitable for application in organic photovoltaic (OPV) cells. Two unsymmetrical squaraines (USQs), namely **BIBISQ** and **TIBISQ**, with two electron-donating aryls directly linked to the electron-withdrawing squaric acid core (Y-manner) could act as high performance donor materials for solution-processed bulk-heterojunction OPV cells. Both of two USQs show ideal low bandgaps (1.47 eV for **BIBISQ** and 1.39 eV for **TIBISQ**) with an intense and broad absorption band in the range of 500-900 nm, and relatively low HOMO levels of ~ -5.10 eV. The BHJ-OPV based on both of them simultaneously show excellent J_{sc} (over 13 mA cm^{-2}), V_{oc} (0.84V), FF (0.49) and PCEs of over 5% under the blend ratio of USQs:PC₇₁BM=1:3. These results are indicating that the two USQs are quite promising candidates for small molecular (SM) OPV and the Y-manner should be quite perspective linked method for USQs.

Keywords squaraine, organic photovoltaic cell, linked manner, increased donor content

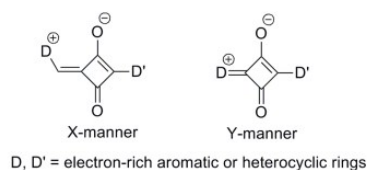
1. Introduction

Owing to its nanometer-scaled phase separation in the donor-acceptor (D-A) blending system thus more efficient D/A interfacial contact, bulk-heterojunction (BHJ) organic photovoltaic (OPV) device has been considered as a promising technique for renewable energy source applications.^{1, 2} In recent decade, small molecular (SM) photovoltaic donor materials have attracted considerable attention for preparing BHJ-OPVs due to their unique advantages over their polymer counterparts, such as well-defined molecular structure and molecular weight, facile synthesis and high purity without batch to batch variations.³ Therefore, many kinds of small molecular photovoltaic donor materials have been developed, including oligothiophenes, dyes, fused acenes, triphenylamine-based molecules and so on.⁴⁻⁸ Up to now, the power conversion efficiency (PCE) of SMOPVs have been achieved as high as >10% with a high donor content (D:A=1:0.8) when employed an oligothiophene derivative (DRCN5T) as donor material.⁹

Recently, squaraines (SQs) have emerged as promising donor materials in OPVs due to their strong and broad absorption band in the visible and near infrared regions.¹⁰⁻¹⁶ As far, the record power conversion efficiency (PCE) of squaraines based BHJ-OPVs is 5.50% with a rather low donor content (D/A ratio is 1:6)¹⁷ and the PCE of tandem devices based on squaraines is up to 8.3%.¹⁸

In recent years, our group has designed a series of USQs in which the D and D' segments are connected to the A subunit directly and via a methyldiene bridge, respectively (X-manner in Scheme 1), and the PCE of these USQs based BHJ-OPV

devices is improved from 1.54% to 4.29%, however, the optimized D/A ratios fall into the region of 1:8~1:5 with a low donor content.¹⁹⁻²² According to the literature reported, the photophysical and chemical properties of squaraines are correlated highly with their connected manners,^{23, 24} which are closely related with their OPV performance. Therefore, very recently, our group has firstly designed some USQs with their two electron-donating aryls linked directly to the electron-withdrawing squaric acid core in Y-manner (Scheme 1).²⁵ The OPV device based on them rendered a short current density (J_{sc}) of up to 12.03 mA cm⁻² and a PCE of 4.35% with a D/A ratio of 1:5. These preliminary results indicated that D and D' linked to A in Y-manner should be quite promising linked manner for USQs donor materials. However, the PCE of them is unsatisfactory due to their relatively low open circuit voltage (V_{oc} , 0.78 V) and fill factor (FF, 0.45). It is noteworthy that one of their donor segments is pyrrole derivative, whose electron-donating ability is much better than phenyl groups, which leads to a relatively high HOMO energy level and then low V_{oc} .



Scheme 1. Two linking manners of photovoltaic USQs derivatives.

Therefore, from these previous results, two novel USQs with Y-manner linked have been designed and synthesized. The phenyl groups, such as *N,N*-dibutylaniline^{16, 26} or 4-(*p*-tolyl)-1,2,3,3a,4,8b-hexahydrocyclopenta[*b*]indole which are the promising groups in OPV donor materials were used to be D subunit;^{20, 27} 5-(8,9,10,10a-tetrahydrobenzo[*e*]cyclopenta[*b*]indol-7(7*aH*)-yl)benzene-1,3-diol, was

chosen to act as D' subunit.²⁵ The molecular structures of two novel USQs (**BIBISQ** and **TIBISQ**) are shown in Scheme 2. Both of two USQs show ideal low bandgaps of 1.47 eV for **BIBISQ** and 1.39 eV for **TIBISQ** with an intense and broad absorption band in the range of 500-900 nm,²⁸ and relatively low HOMO levels of ~ -5.10 eV. The BHJ-SMOPV based on both of them simultaneously show enhanced V_{oc} (0.84V) and FF (0.49). Meanwhile, the excellent J_{sc} of over 13 mA cm^{-2} is achieved due to the relatively high content of USQs (USQs:PC₇₁BM=1:3). Ultimately, the PCEs of BHJ-SMOPV based on USQs are over 5%. Especially, the BHJ-SMOPV based on the **TIBISQ** shows a high J_{sc} of up to 13.50 mA cm^{-2} and an excellent PCE of 5.49%, which could compare to the highest J_{sc} ²⁹ and PCE^{17, 30, 31} among all the reported squaraine based BHJ-OPV cells. These results indicate that Y-manner is indeed a quite promising linking way for the construction of high performance OPV USQs.

2. Materials and methods

2.1. Instruments and characterization

¹H and ¹³C NMR spectra were recorded on a Bruker Avance AV II-400 MHz instrument with tetramethylsilane as internal standard. High resolution mass spectra were measured on a Shimadzu LCMS-IT-TOF. The purity of the two USQs were measured by EZChrom Elite for Hitachi high performance liquid chromatography (DAD and RI detector). Absorption spectra of two USQs in $5 \times 10^{-6} \text{ mol L}^{-1}$ chloroform solution and thin film states were measured with a Perkin Elmer Lambda 950 UV-Vis scanning spectrophotometer.

2.2. Electrochemistry measurement

Cyclic voltammetry was performed in 0.10 mol L⁻¹ tetrabutylammonium perchlorate/anhydrous dichloromethane (2.5×10⁻⁴ mol L⁻¹) with a LK 2010 electrochemical work station, using a three-electrode cell with a Pt disk working electrode, a Pt wire counter electrode and a Ag/AgNO₃ (0.1 mol L⁻¹ in acetonitrile) reference electrode. Solutions have been pre-degassed by argon bubbling for 30 min prior to each experiment. At the end of each measurement, ferrocenium/ferrocene redox couple was added as an internal potential reference.

2.3. Preparation of organic photovoltaic cells

Photovoltaic devices were fabricated on indium-tin oxide (ITO) coated-glass substrate (sheet resistance = 15 Ω sq⁻¹) with a layered structure of ITO/ MoO₃ (8 nm)/ USQs:PC₇₁BM (60 nm)/ BCP (6 nm)/ Al (100 nm). The patterned ITO-coated glass substrates were cleaned through sequential sonication in detergent, deionized water, acetone and isopropanol for 20 min each. The cleaned substrates were dried in an oven at 65 °C for 12 h before using. The substrate was treated by UV-ozone for 30 min, then immediately transferred into a high vacuum chamber for deposition of 8 nm MoO₃ at pressure of less than 1×10⁻⁴ Pa with a rate of 0.2 Å s⁻¹. Subsequently, the photoactive layer (thickness: 60±5 nm) was fabricated by spin-casting a blend of the USQs and PC₇₁BM in chloroform solution with total concentration of 20 mg mL⁻¹ (3500 rpm, 45 s) under a N₂-filling glove box at 25 °C. Finally, the substrates were transferred back to the high-vacuum chamber, where BCP (6 nm) and Al (100 nm) were deposited as the top electrode at pressures of less than 2×10⁻⁴ Pa with a rate of

0.20 \AA s^{-1} and 2.0~3.0 \AA s^{-1} , respectively. The active area of OPV cells is 9 mm^2 . To obtain the average data related to device performance, several batches of devices (4 cells per batch) for each set of conditions were fabricated and tested. Current density-voltage (J - V) and external quantum efficiency (EQE) characterization of organic photovoltaic cells were performed on a CEP-2000 integrated system manufactured by Bunkoukeiki Co. The integration of EQE data over a AM 1.5G solar spectrum yielded calculated J_{sc} values with an experimental variation of less than 5% was relative to the J_{sc} measured under 100 mW cm^{-2} simulated AM 1.5G light illumination. Hole-only devices were fabricated with the structures of ITO/ MoO₃ (8 nm)/ USQs:PC₇₁BM (60 nm)/ MoO₃ (8 nm)/ Al (100 nm).

Samples for atomic force microscopy (AFM) measurements were prepared by spin-casting from USQs:PC₇₁BM=1:3 in chloroform solution on glass substrates.

2.4. Synthesis

The synthetic routes of intermediates and target molecules USQs are outlined in Scheme 2. Compounds **1-9** were prepared according to the procedures described in the literatures.^{25, 27, 32, 33} *n*-Butanol and toluene were distilled from sodium freshly prior to use. All the other chemicals, reagents, and solvents were used as received from the suppliers.

2.4.1 *N,N*-dibutylaniline (**1**)

A mixture of aniline (5 mL, 52.63 mmol), *n*-C₄H₉Br (17 mL, 157.89 mmol) and Na₂CO₃ (22.37 g, 210.53 mmol) in 25 mL of 9:1 v/v dimethylformamide (DMF)/*N*-methylpyrrolidinone (NMP) was heated at 120 °C for 12 h. The reaction

mixture was then cooled to room temperature and filtered to remove the insoluble material. The precipitate was washed with ethyl acetate, and the combined filtrate was evaporated to dryness. Water was added, and the aqueous phase was extracted with ethyl acetate. After silica gel column chromatography (hexane), a pale yellow oil (9.18 g, 85%) was obtained.

2.4.2 4-(*p*-Tolyl)-1,2,3,3a,4,8b-hexahydrocyclopenta[*b*]indole (3)

A mixture of compound **2** (0.80 g, 5.02 mmol), 1-bromo-4-methylbenzene (0.86 g, 5.02 mmol), NaOBu-*t* [sodium *tert*-butoxide] (0.72 g, 7.53 mmol), Pd(OAc)₂ [palladium (II) acetate] (34 mg, 3%), and P(*t*-Bu)₃HBF₄[tri(*tert*-butyl)phosphine tetrafluoroborate] (73 mg, 5%) in anhydrous toluene (50 mL) was refluxed under Ar for 6 h. After cooled down, the reaction mixture was filtered, and the filtrate was concentrated in vacuo. The resulting crude product was purified by silica gel column chromatography (hexane) to give **3** (0.86 g, 70%) as colorless oil. ¹HNMR (400 MHz, CDCl₃, ppm) δ 7.20 (d, *J* = 8.4 Hz, 2H, ArH), 7.15 (d, *J* = 8.4 Hz, 2H, ArH), 7.12 (d, *J* = 7.2 Hz, 1H, ArH), 7.05 (t, *J* = 8.0 Hz, 1H, ArH), 6.93 (d, *J* = 8.0 Hz, 1H, ArH), 6.72 (t, *J* = 7.2 Hz, 1H, ArH), 4.77 (t, *J* = 8.8 Hz, 1H, CH), 3.84 (t, *J* = 8.8 Hz, 1H, CH), 2.33 (s, 3H, CH₃), 2.08-1.99 (m, 1H, CH₂), 1.95-1.84 (m, 2H, CH₂), 1.82-1.75 (m, 1H, CH₂), 1.70-1.60 (m, 1H, CH₂), 1.59-1.47 (m, 1H, CH₂).

2.4.3 3-Chloro-4-(4-(*di*butylamino)phenyl)cyclobut-3-ene-1,2-dione (5)

The mixture of squaryl chloride **4** (1.00 g, 6.67 mmol), *N,N*-dibutylaniline **1** (1.37 g,

6.67 mmol) in dried toluene (50 mL) was refluxing for 5 h, then the reaction mixture was cooled and evaporated under vacuum. The residue was purified by silica gel column chromatography (hexane/dichloromethane=2:1) to give **5** (0.71 g, 30%) as yellow solid. ¹HNMR (400 MHz, CDCl₃, ppm) δ 8.15 (d, *J* = 9.2 Hz, 2H, ArH), 6.75 (d, *J* = 9.2 Hz, 2H, ArH), 3.44 (t, *J* = 7.6 Hz, 4H, CH₂), 1.69-1.61 (m, 4H, CH₂), 1.46-1.37 (m, 4H, CH₂), 1.03 (t, *J* = 7.2 Hz, 6H, CH₃).

2.4.4 3-Chloro-4-(4-(*p*-tolyl)-1,2,3,3a,4,8b-hexahydrocyclopenta[*b*]indol-7-yl)cyclobut-3-ene-1,2-dione (**6**)

The mixture of squaryl chloride **4** (0.40 g, 2.65 mmol), **3** (0.60 g, 2.41 mmol) in dried toluene (30 mL) was refluxing for 5 h, then the reaction mixture was cooled and evaporated under vacuum. The residue was purified by silica gel column chromatography (hexane/dichloromethane=2:1) to give **6** (0.22 g, 25%) as orange solid. ¹HNMR (400 MHz, CDCl₃, ppm) δ 8.01 (d, *J* = 8.4 Hz, 1H, ArH), 7.96 (s, 1H, ArH), 7.26-7.16 (m, 4H, ArH), 6.74 (d, *J* = 8.8 Hz, 1H, ArH), 4.99 (t, *J* = 8.4 Hz, 1H, CH), 3.89 (t, *J* = 8.4 Hz, 1H, CH), 2.38 (s, 3H, CH₃), 2.14-2.01 (m, 1H, CH₂), 1.92-1.85 (m, 2H, CH₂), 1.76-1.66 (m, 2H, CH₂), 1.56-1.44 (m, 1H, CH₂).

2.4.5 3-*N,N*-(dibutylamino)phenyl-4-hydroxy-3-cyclobutene-1,2-dione (**7**)

5 (0.71 g 2.22 mmol) was dissolved in a mixture of acetic acid (30 mL), concentrated hydrochloric acid (4 mL) and water (10 mL). This mixture was refluxed for 2 h, and cooled to room temperature. Water (200 mL) was added dropwise into the

mixture, then the yellow precipitate **7** (0.59 g, 88%) was obtained by filtration, washed with ether and dried. ^1H NMR (400 MHz, $\text{DMSO}-d_6$, ppm) δ 7.86 (s, 2H, ArH), 6.81 (s, 2H, ArH), 3.38 (s, 4H, CH_2), 1.49 (s, 4H, CH_2), 1.34-1.23 (m, 4H, CH_2), 0.92 (t, $J = 6.8$ Hz, 6H, CH_3).

2.4.6 3-Hydroxy-4-(4-(*p*-tolyl)-1,2,3,3a,4,8b-hexahydrocyclopenta[*b*]indol-7-yl)cyclobut-3-ene-1,2-dione (**8**)

6 (0.22 g, 0.60 mmol) was dissolved in a mixture of acetic acid (15 mL), concentrated hydrochloric acid (2 mL) and water (5 mL). This mixture was refluxed for 6 h, and cooled to room temperature. Water (100 mL) was added dropwise into the mixture, then the brown precipitate **8** (0.20 g, 90%) was obtained by filtration, washed with ether and dried. ^1H NMR (400 MHz, $\text{DMSO}-d_6$, ppm) δ 7.74 (s, 1H, ArH), 7.72 (d, $J = 8.8$ Hz, 1H, ArH), 7.26 (d, $J = 8.4$ Hz, 2H, ArH), 7.23 (d, $J = 8.4$ Hz, 2H, ArH), 6.85 (d, $J = 8.4$ Hz, 1H, ArH), 4.99 (t, $J = 6.4$ Hz, 1H, CH), 3.87 (t, $J = 8.4$ Hz, 1H, CH), 2.30 (s, 3H, CH_3), 2.11-2.02 (m, 1H, CH_2), 1.80-1.60 (m, 4H, CH_2), 1.43-1.33 (m, 2H, CH_2).

2.4.7 4-(4-(Dibutyliminio)cyclohexa-2,5-dien-1-ylidene)-2-(2,6-dihydroxy-4-(8,9,10,10a-tetrahydrobenzo[*e*]cyclopenta[*b*]indol-7(7aH)-yl)phenyl)-3-oxocyclobut-1-enolate (**BIBISQ**)

A mixture of compound **9** (0.17 g, 0.53 mmol) and **7** (0.16 g, 0.53 mmol) in butanol (4 mL) and toluene (12 mL) was refluxed at 140°C under Ar for 12 h. Then the

reaction mixture was concentrated in vacuo, and the crude product was purified by column chromatography (dichloromethane) and followed by recrystallization from dichloromethane/methanol to give green shiny crystals of **BIBISQ** (0.25 g, 78%). Purity: 100% (HPLC, eluent: THF/CH₃OH=1:9). m.p. 219-221 °C. ¹HNMR (400 MHz, CDCl₃, ppm) δ 12.84 (s, 2H, OH), 8.15 (d, *J* = 8.8 Hz, 2H, ArH), 7.87 (d, *J* = 8.0 Hz, 1H, ArH), 7.83 (d, *J* = 8.4 Hz, 1H, ArH), 7.79 (d, *J* = 9.2 Hz, 1H, ArH), 7.71 (d, *J* = 8.8 Hz, 1H, ArH), 7.53 (t, *J* = 7.2 Hz, 1H, ArH), 7.44 (t, *J* = 7.2 Hz, 1H, ArH), 7.09 (s, 2H, ArH), 6.40 (s, 2H, ArH), 4.98-4.93 (m, 1H, CH), 4.39-4.34 (m, 1H, CH), 3.44 (t, *J* = 7.6 Hz, 4H, CH₂), 2.39-2.25 (m, 2H, CH₂), 2.12-1.99 (m, 2H, CH₂), 1.79-1.67 (m, 4H, CH₂), 1.58-1.49 (m, 2H, CH₂), 1.44-1.35 (m, 4H, CH₂), 0.99 (t, *J* = 7.2 Hz, 6H, CH₃). ¹³CNMR (100 MHz, CDCl₃, ppm) δ 182.8, 178.1, 166.5, 164.6, 155.2, 152.6, 140.1, 132.5, 130.9, 130.7, 130.1, 128.8, 128.6, 126.9, 124.5, 123.3, 117.8, 115.2, 112.3, 108.0, 97.0, 69.7, 51.2, 44.7, 35.1, 33.3, 29.6, 24.8, 20.2, 13.9. HRMS (ESI)⁺ *m/z*: [M+H]⁺ calcd. for C₃₉H₄₁N₂O₄, 601.3061; found, 601.3062. Anal. Calcd for C₃₉H₄₀N₂O₄: C, 77.97; H, 6.71; N, 4.66. Found: C, 78.11; H, 6.94; N, 5.12.

2.4.8 2-(2,6-Dihydroxy-4-(8,9,10,10a-tetrahydrobenzo[e]cyclopenta[b]indol-7(7aH)-yl)phenyl)-4-(4-(*p*-tolyl)-1,3,3a,8b-tetrahydrocyclopenta[b]indol-4-ium-7(2H)-ylidene)-3-oxocyclobut-1-enolate (TIBISQ)

A mixture of compound **9** (0.18 g, 0.58 mmol) and **8** (0.20 g, 0.58 mmol) in butanol (4 mL) and toluene (12 mL) was refluxed at 140°C under Ar for 12 h. Then the reaction mixture was concentrated in vacuo, and the crude product was purified by

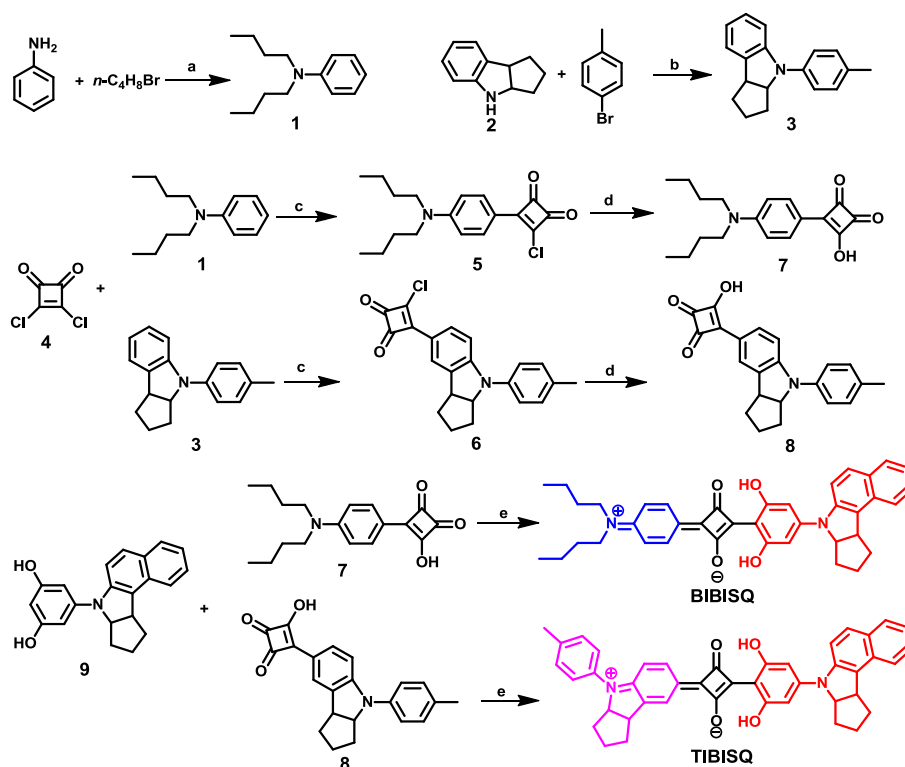
column chromatography (dichloromethane) and followed by recrystallization from dichloromethane/methanol to give green shiny crystals of **TIBISQ** (0.27 g, 73%). Purity: 99.0% (HPLC, eluent: THF/CH₃OH=1:9). m.p. 248-249 °C. ¹HNMR (400 MHz, CDCl₃, ppm) δ 12.69 (s, 2H, OH), 8.02 (d, *J* = 8.4 Hz, 1H, ArH), 7.97 (s, 1H, ArH), 7.84 (d, *J* = 8.4 Hz, 1H, ArH), 7.79 (d, *J* = 8.4 Hz, 1H, ArH), 7.75 (d, *J* = 8.8 Hz, 1H, ArH), 7.69 (d, *J* = 8.8 Hz, 1H, ArH), 7.52 (t, *J* = 7.2 Hz, 1H, ArH), 7.40 (t, *J* = 7.2 Hz, 1H, ArH), 7.26 (d, *J* = 8.0 Hz, 2H, ArH), 7.20 (d, *J* = 8.4 Hz, 2H, ArH), 6.75 (d, *J* = 8.0 Hz, 1H, ArH), 6.38 (s, 2H, ArH), 4.98 (s, 1H, CH), 4.91 (s, 1H, CH), 4.32 (s, 1H, CH), 3.85 (s, 1H, CH), 2.39 (s, 3H, CH₃), 2.36-2.19 (m, 2H, CH₂), 2.12-1.84 (m, 5H, CH₂), 1.77-1.66 (m, 3H, CH₂), 1.57-1.45 (m, 2H, CH₂). ¹³CNMR (100 MHz, CDCl₃, ppm) δ 182.9, 177.6, 165.8, 164.5, 155.1, 154.5, 140.1, 136.9, 136.8, 135.7, 133.1, 130.9, 130.8, 130.3, 130.1, 128.8, 128.6, 126.9, 126.2, 124.5, 123.3, 123.2, 120.6, 115.2, 108.1, 108.0, 97.0, 70.9, 69.7, 44.7, 44.4, 35.5, 35.1, 33.3, 32.8, 24.8, 24.0, 21.1. HRMS (ESI)⁺ *m/z*: [M+H]⁺ calcd. for C₄₃H₃₇N₂O₄, 645.2748; found, 645.2748. Anal. Calcd for C₄₃H₃₆N₂O₄: C, 80.10; H, 5.63; N, 4.34. Found: C, 80.52; H, 5.74; N, 4.82.

3. Results and discussion

3.1 Synthesis and characterization

The synthetic routes of intermediates and target molecules USQs are outlined in Scheme 2. Compounds **1-9** were prepared according to the procedures described in the literatures.^{25, 27, 32, 33} The two objective molecules **BIBISQ** and **TIBISQ** were

prepared by condensation of **9** with **7** and **8**, respectively. The molecular structures of the USQs were characterized by ^1H NMR, ^{13}C NMR, HR-ESIMS and element analysis. The purity of both two USQs is conformed to be >99.0% by HPLC analysis.



Scheme 2. Synthetic routes of two USQs. (a) Na_2CO_3 (4.0 equ.), dimethylformamide (DMF)/*N*-methylpyrrolidinone (NMP)=9:1 (v/v), 120 °C, 12 h, 85%; (b) $\text{NaOBu-}t$ (1.5 equ.), $\text{Pd}(\text{OAc})_2$ (3% equ.), $\text{P}(t\text{-Bu})_3\text{HBF}_4$ (5% equ.), anhydrous toluene, reflux under Ar, 6 h, 70%; (c) anhydrous toluene, reflux under Ar, 5 h, 30% for **5** and 25% for **6**; (d) acetic acid/water=3:1 (v/v), concentrated HCl, reflux, 2-6 h, 88% for **7** and 90% for **8**; (e) *n*-butanol/toluene=1:3 (v/v), 140° C under Ar, 12 h, 78% for **BIBISQ** and 73% for **TIBISQ**.

3.2 Optical properties

The UV-Vis absorption spectra of **BIBISQ** and **TIBISQ** in dilute chloroform solution and thin solid films (spin-casted from chloroform solution) are shown in **Fig.**

1, and the relative data are summarized in **Table 1**. In solution, analogous to most of squaraines,^{19-22, 25} both the two compounds show intense absorption (molar extinction coefficient $> 10^5 \text{ M}^{-1} \text{ cm}^{-1}$) in Vis-NIR regions. The λ_{max} of **BIBISQ** and **TIBISQ** are 691 nm and 713 nm, respectively, with full width at half maxima (FWHM) of 53 nm or 61 nm. In thin film state, both the two compounds display drastically red-shifted and broadened absorption bands (λ_{max} : 748 nm for **BIBISQ**, 760 nm for **TIBISQ**; FWHM: 184 nm for **BIBISQ**, 217 nm for **TIBISQ**). This should be attributed to their intense intermolecular interactions in condensed state. The intense and wide absorption band of the two compounds in 500-900 nm should be beneficial to the harvesting of sunlight hence the enhancement of J_{sc} of their OPV devices. Through the absorption spectra of their solid film samples, the optical bandgap of **BIBISQ** and **TIBISQ** is estimated to be 1.47 eV and 1.39 eV, respectively, which is an ideal value for photovoltaic donor materials.²⁸

Table 1. Optical and electrochemical properties of the two USQs.

Compound	λ_{abs}^a (nm)	λ_{abs}^b (nm)	FWHM (nm)		E_g^{opt} (eV)	E_{ox} (V)	HOMO ^c (eV)	LUMO ^d (eV)
	(log ϵ)		Solution	Film				
BIBISQ	691 (5.32)	748	53	184	1.47	0.32	-5.12	-3.65
TIBISQ	713 (5.50)	760	61	217	1.39	0.28	-5.08	-3.69

^a Measured in dilute chloroform solution ($5.00 \times 10^{-6} \text{ M}$); ^b measured in thin film state; ^c HOMO = $(-4.80 - E_{\text{ox}}) \text{ eV}$; ^d LUMO = $E_g^{\text{opt}} + \text{HOMO}$.

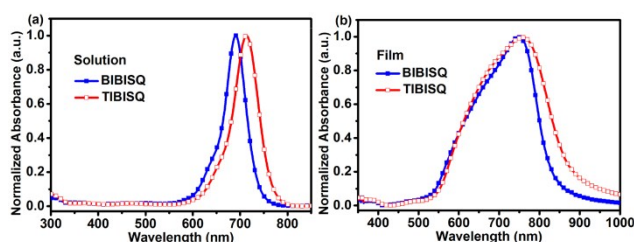
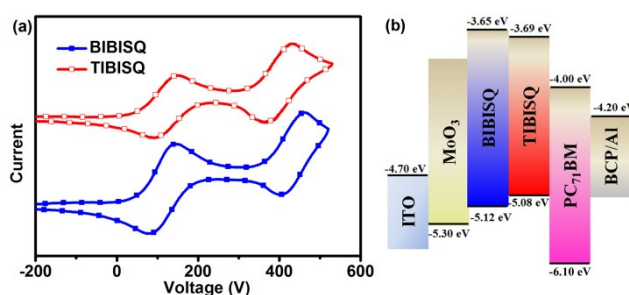


Fig.1. Absorption spectra of two USQs in solution (a) and thin films (b).

3.3 Electrochemical properties

Cyclic voltammetry experiments were carried out on **BIBISQ** and **TIBISQ** in dichloromethane solution with tetrabutylammonium perchlorate as the supporting electrolyte, and the results are shown in **Table 1** and **Fig. 2**. The HOMO level of **BIBISQ** and **TIBISQ** is estimated to be -5.12 eV and -5.08 eV respectively by comparing the oxidation wave peak of the compounds with Fc/Fc^+ redox couple whose energy level is 4.80 eV below vacuum.¹⁵ And the corresponding LUMO energy level of **BIBISQ** and **TIBISQ** is calculated to be -3.65 eV and -3.69 eV, respectively through their HOMO level and optical bandgap data.³⁴ From these results, we can roughly guess the V_{oc} of BHJ-OPVs based on these two USQs and PC_{71}BM may be in 0.7 - 0.9 V.³⁵

**Fig. 2.** Cyclic voltammograms of the two USQs (a) and the energy levels of the components for OPV devices (b).

3.4 Photovoltaic characteristics

To evaluate their photovoltaic performance, BHJ-OPV cells with **BIBISQ** or **TIBISQ** as electron donor material and [6,6]-phenyl- C_{71} butyric acid methyl ester (PC_{71}BM) as electron acceptor material have been fabricated with different D/A

blending ratios. The device structure is ITO/MoO₃ (8 nm)/USQs:PC₇₁BM (60 nm)/BCP (6 nm)/ Al (100 nm). The corresponding data and curves are shown in **Table 2**, **Fig. 3** and **4**. The results indicate that similar trend in photovoltaic performance of OPV devices based on both **BIBISQ** and **TIBISQ** could be observed when their D/A ratio varies from 1:1 to 1:8. Taking **TIBISQ** as an example, when the blend ratio is changed from 1:1 to 1:8, the V_{oc} and FF of the corresponding BHJ-OPV devices are nearly unaltered, while the J_{sc} is found to show distinct variation, which matches with the corresponding EQE spectra of the devices. As shown in **Fig 3b**, in the EQE spectra of **TIBISQ**-devices, three major bands could be identified, with their peaks approximately located at 380 nm, 480 nm and 760 nm, respectively. The first two high-energy bands should stem from the absorption of PC₇₁BM; and the third low-energy band at ~760 nm should arise from the absorption of **TIBISQ**. With the increasing composition of **TIBISQ**, the intensity of the third band peaked at ~760 nm increases gradually, which is consistent with the corresponding absorption spectrum of D/A blend film with similar D/A mixing ratio (shown in **Fig. 3c**). Accordingly, with increasing D/A ratio from 1:8 to 1:3, the J_{sc} of **TIBISQ**-device increases gradually from 10.92 to 13.02 mA cm⁻². However, in the case of **TIBISQ**-device with D/A ratio of 1:1, the intensity of the third band in its EQE spectrum decreases rather than increased drastically, despite the fact that the 1:1 blend film displays the strongest absorption at this band, as shown in **Fig. 3c**. This may ascribed to the drastically different morphology of the blend films between 1:1 and other D/A ratios (vide **Fig. 5**). Similarly, for **BIBISQ**-devices, the optimized D/A ratio is also found to be 1:3.

Therefore, taking advantage of the more effective absorption in the NIR region due to the increased content of USQ in the 1:3 optoelectronic film, the resulting devices could both show impressive J_{sc} of $\sim 13 \text{ mA cm}^{-2}$, which is much higher than that of the reported USQ-based BHJ-SMOPVs.^{15, 25} Additionally, according to the experimental and calculation results (**Fig. 6**), the hole mobility of the as-prepared 1:3 D/A blending films is relatively high (3.25×10^{-5} and $6.21 \times 10^{-5} \text{ cm}^2 \text{ V}^{-1} \text{ s}^{-1}$ for **BIBISQ**- and **TIBISQ**-based film in sequence), which would also contribute to the high J_{sc} and FF,³⁶ hence high PCE of 4.97%~5.08% of the devices.

Table 2. Photovoltaic performance of USQs-OPV devices.

Active layer (w/w)	V_{oc} (V)	J_{sc} (mA/cm ²)	FF	PCE (%) ^b
TIBISQ:PC ₇₁ BM=1:1	0.83	9.95	0.45	3.72 (3.65)
TIBISQ:PC ₇₁ BM=1:3	0.83	13.02	0.47	5.08 (5.03)
TIBISQ:PC ₇₁ BM=1:5	0.84	11.15	0.50	4.68 (4.57)
TIBISQ:PC ₇₁ BM=1:8	0.84	10.92	0.48	4.40 (4.32)
TIBISQ:PC ₇₁ BM=1:3 ^a	0.83	13.50	0.49	5.49 (5.39)
BIBISQ:PC ₇₁ BM=1:1	0.83	8.23	0.43	2.94 (2.81)
BIBISQ:PC ₇₁ BM=1:3	0.84	12.87	0.46	4.97 (4.92)
BIBISQ:PC ₇₁ BM=1:5	0.85	10.97	0.49	4.57 (4.46)
BIBISQ:PC ₇₁ BM=1:8	0.86	10.41	0.47	4.21 (4.13)
BIBISQ:PC ₇₁ BM=1:3 ^a	0.83	13.13	0.49	5.34 (5.24)

^a Thermal annealed at 80 °C for 10 min; ^b the average PCEs are provided in parentheses.

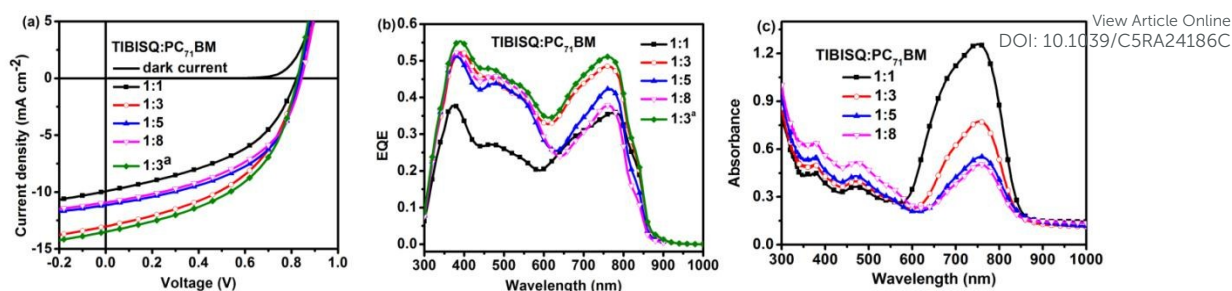


Fig. 3. The *J-V* characteristics (a), EQE characteristics (b) of the TIBISQ devices; and absorption spectra (c) of the photoactive layers with different D/A ratios.

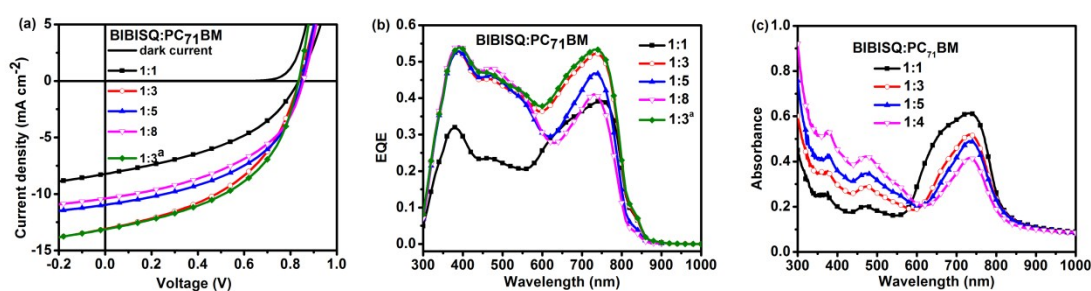


Fig. 4. The *J-V* characteristics (a), EQE characteristics (b) of the OPV devices and absorption spectrum (c) of the blend films with the different blend ratios of BIBISQ:PC₇₁BM.

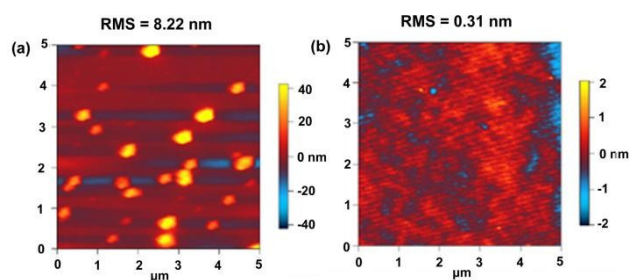


Fig. 5. Tapping-mode AFM height images (5 × 5 μm) of TIBISQ:PC₇₁BM blend films with different ratio (a, 1:1; b, 1:3).

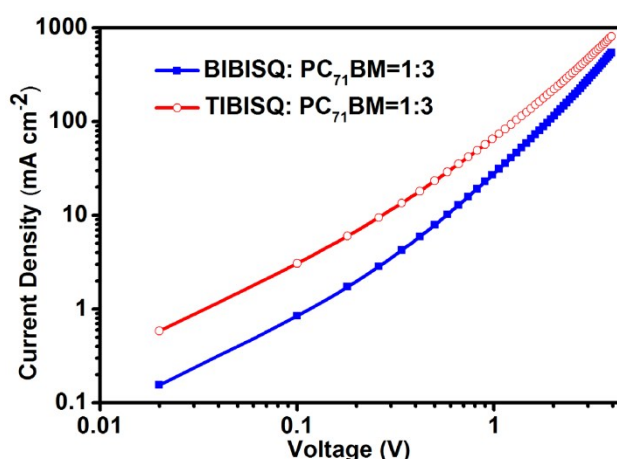


Fig. 6. Current density-voltage characteristics of hole-only single-carrier devices using USQs:PC₇₁BM=1:3 blend films as active layer

Upon thermal annealing (80 °C, 10 min), the device performance of both **BIBISQ** and **TIBISQ** is observed to be enhanced, with PCE of 5.34% and 5.49%, respectively. The enhanced PCEs should be attributed not only to the improved J_{sc} (for **BIBISQ**, from 12.87 to 13.13 mA cm⁻²; for **TIBISQ**, from 13.02 to 13.50 mA cm⁻²) which is consistent with their EQE measurement results (shown in **Fig. 3b** and **Fig. 4b**), but also to the enhanced FF (for **BIBISQ**, from 0.46 to 0.49; for **TIBISQ**, from 0.47 to 0.49). Moreover, the impressive J_{sc} (13.50 mA cm⁻²) and excellent PCE (5.49%) of **TIBISQ**-based BHJ-OPV could compare to the highest J_{sc} ²⁹ and PCE^{17, 30, 31} among all the reported squaraine based BHJ-OPV cells. These results indicate that the Y-mannered molecular backbone is indeed quite promising for the construction of perspective OPV USQs with increased donor content in photoactive layer.

It is worthwhile to mention that the optimized D/A composite ratio in these devices based on two USQs is 1:3. Generally, a larger content of donor material in the blend film is propitious to the harvesting of sunlight hence the enhancement of PCE of the device,³⁷ therefore, the typical D/A ratio in highly efficient OPV devices lies in the

range of 1:1~1:2.⁹ However, although many D/A composite ratio has been employed in the BHJ OPV devices based on squaraines, the record PCE of 5.50% for BHJ-OPV using symmetrical squaraines (SSQs, D-A-D-type) could be achieved with a rather low D/A ratio (1:6) according to Wei's report.¹⁷ Similarly, for our reported USQs donor materials, the optimized D/A ratios fall into the region of 1:8~1:5.¹⁹⁻²² The low content of donor material in photoactive layer may hamper the photovoltaic performance of these squaraine materials. Therefore, the present investigation shows the much enhanced content of USQ donor materials in active layers (the optimized D/A ratios of BHJ-OPVs based on **BIBISQ** and **TIBISQ** are both 1:3) is beneficial to absorb more solar light in the NIR region, which contributes to the impressive J_{sc} over 13 mA cm^{-2} and PCE over 5% of BHJ-OPVs, which would open a more confident way to improve OPV performances of squaraine materials by molecular tailoring.

4. Conclusion

In conclusion, two novel USQs bearing Y-manner molecular platform have been developed. Both of them show relatively low bandgap of $< 1.5 \text{ eV}$, intense and wide absorption band in 500-900 nm, and relatively low HOMO energy level of $\sim -5.10 \text{ eV}$ as well. BHJ-OPV devices based on them could show relatively high V_{oc} of 0.84 V, rather impressive J_{sc} of over 13 mA cm^{-2} and high FF of 0.49, consequently high PCE of over 5.0% even at a relatively high donor content (the optimized D/A ratio is 1:3). Consequently, Y-manner is indeed a quite promising linking way for the construction of high performance OPV USQs in terms of increased donor content.

Acknowledgments

We acknowledge the financial support for this work by the National Natural Science Foundation of China (project No. 21190031, 21372168 and 21432005), Fujian Key Laboratory of Polymer Materials (Fujian Normal University) (FJKL-POLY 201502) and China Scholarship Council. We are grateful to the Comprehensive Training Platform of Specialized Laboratory, College of Chemistry, Sichuan University for providing NMR and HR-MS data for the intermediates and objective compounds.

Notes and references

^a *Key Laboratory of Green Chemistry and Technology (Ministry of Education), College of Chemistry, Sichuan University, Chengdu 610064, P. R. China. E-mail: huangyan@scu.edu.cn, luzhiyun@scu.edu.cn*

^b *Department of Organic Device Engineering, Yamagata University, 4-3-16 Jonan, Yonezawa, Yamagata 992-8510, Japan. Email: h-sasabe@yz.yamagata-u.ac.jp.*

†Electronic Supplementary Information (ESI) available: The ¹H NMR, ¹³C NMR and HRMS spectra of **BIBISQ** and **TIBISQ**.

‡ The first two authors contributed equally to this work.

1. A. J. Heeger, *Adv. Mater.*, 2014, **26**, 10-27.
2. Y. Huang, E. J. Kramer, A. J. Heeger and G. C. Bazan, *Chem. Rev.*, 2014, **114**, 7006-7043.

3. J. Roncali, P. Leriche and P. Blanchard, *Adv. Mater.*, 2014, **26**, 3821-3838.
4. Y. Lin, Y. Li and X. Zhan, *Chem. Soc. Rev.*, 2012, **41**, 4245-4272.
5. A. Mishra and P. B. Auerle, *Angew. Chem. Int. Ed.*, 2012, **51**, 2020-2067.
6. P. Gautam, R. Misra, S. A. Siddiqui and G. D. Sharma, *ACS Appl. Mater. Interfaces*, 2015, **7**, 10283-10292.
7. P. Gautam, R. Misra, S. A. Siddiqui and G. D. Sharma, *Org. Electron.*, 2015, **19**, 76-82.
8. T. Jadhav, R. Misra, S. Biswas and G. D. Sharma, *Phys. Chem. Chem. Phys.*, 2015, **17**, 26580-26588.
9. B. Kan, M. Li, Q. Zhang, F. Liu, X. Wan, Y. Wang, W. Ni, G. Long, X. Yang, H. Feng, Y. Zuo, M. Zhang, F. Huang, Y. Cao, T. P. Russell and Y. Chen, *J. Am. Chem. Soc.*, 2015, **137**, 3886-3893.
10. G. Chen, H. Sasabe, W. Lu, X. Wang, J. Kido, Z. Hong and Y. Yang, *J. Mater. Chem. C.*, 2013, **1**, 6547-6552.
11. Y. Fu, D. A. da Silva Filho, G. Sini, A. M. Asiri, S. G. Aziz, C. Risko and J. Brédas, *Adv. Funct. Mater.*, 2014, **24**, 3790-3798.
12. G. Chen, H. Sasabe, T. Igarashi, Z. Hong and J. Kido, *J. Mater. Chem. A.*, 2015, **3**, 14517-14534.
13. H. Sasabe, T. Igarashi, Y. Sasaki, G. Chen, Z. Hong and J. Kido, *RSC Adv.*, 2014, **4**, 42804-42807.
14. J. Huang, T. Goh, X. Li, M. Y. Sfeir, E. A. Bielinski, S. Tomasulo, M. L. Lee, N. Hazari and A. D. Taylor, *Nat. Photonics.*, 2013, **7**, 479-485.

15. S. So, H. Choi, H. M. Ko, C. Kim, S. Paek, N. Cho, K. Song, J. K. Lee and J. Ko, *Sol. Energ. Mater. Sol. C.*, 2012, **98**, 224-232.
16. S. Wang, L. Hall, V. V. Diev, R. Haiges, G. Wei, X. Xiao, P. I. Djurovich, S. R. Forrest and M. E. Thompson, *Chem. Mater.*, 2011, **23**, 4789-4798.
17. G. Wei, S. Wang, K. Sun, M. E. Thompson and S. R. Forrest, *Adv. Energy Mater.*, 2011, **1**, 184-187.
18. J. D. Zimmerman, B. E. Lassiter, X. Xiao, K. Sun, A. Dolocan, R. Gearba, D. A. V. Bout, K. J. Stevenson, P. Wickramasinghe, M. E. Thompson, S. R. Forrest, *ACS Nano.*, 2013, **7**, 9268-9275.
19. D. Yang, Y. Zhu, Y. Jiao, L. Yang, Q. Yang, Q. Luo, X. Pu, Y. Huang, S. Zhao and Z. Lu, *RSC Adv.*, 2015, **5**, 20724-20733.
20. L. Yang, Q. Yang, D. Yang, Q. Luo, Y. Zhu, Y. Huang, S. Zhao and Z. Lu, *J. Mater. Chem. A.*, 2014, **2**, 18313-18321.
21. D. Yang, Q. Yang, L. Yang, Q. Luo, Y. Chen, Y. Zhu, Y. Huang, Z. Lu and S. Zhao, *Chem. Commun.*, 2014, **50**, 9346-9348.
22. D. Yang, Q. Yang, L. Yang, Q. Luo, Y. Huang, Z. Lu and S. Zhao, *Chem. Commun.*, 2013, **49**, 10465-10467.
23. I. A. Karpenko, A. S. Klymchenko, S. Gioria, R. Kreder, I. Shulov, P. Villa, Y. Médy, M. Hiberta and D. Bonnet, *Chem. Commun.*, 2015, **51**, 2960-2963.
24. C. Gude and W. Rettig, *J. Phys. Chem. A.*, 2000, **104**, 8050-8057.
25. Y. Chen, Y. Zhu, D. Yang, Q. Luo, L. Yang, Y. Huang, S. Zhao and Z. Lu, *Chem. Commun.*, 2015, **51**, 6133-6136.

26. G. Chen, H. Sasabe, Y. Sasaki, H. Katagiri, X. Wang, T. Sano, Z. Hong, Y. Yang and J. Kido, *Chem. Mater.*, 2014, **26**, 1356-1364.
27. N. F. Montcada, L. Cabau, C. V. Kumar, W. Cambarau and E. Palomares, *Org. Electron.*, 2015, **20**, 15-23.
28. X. Liu, Y. Sun, B. B. Hsu, A. Lorbach, L. Qi, A. J. Heeger and G. C. Bazan, *J. Am. Chem. Soc.*, 2014, **136**, 5697-5708.
29. S. Spencer, H. Hu, Q. Li, H. Ahn, M. Qaddoura, S. Yao, A. Ioannidis, K. Belfield and C. J. Collison, *Prog. Photovolt: Res. Appl.*, 2014, **22**, 488-493.
30. D. Yang, Y. Jiao, L. Yang, Y. Chen, S. Mizoi, Y. Huang, X. Pu, Z. Lu, H. Sasabe and J. Kido, *J. Mater. Chem. A.*, 2015, **3**, 17704-17712.
31. D. Yang, L. Yang, Y. Huang, Y. Jiao, T. Igarashi, Y. Chen, Z. Lu, X. Pu, H. Sasabe and J. Kido, *ACS Appl. Mater. Interfaces.*, 2015, **7**, 13675-13684.
32. W. Wang, A. Fu, J. You, G. Gao, J. Lan and L. Chen, *Tetrahedron.*, 2010, **66**, 3695-3701.
33. D. Yang, Z. Guan, L. Yang, Y. Huang, Q. Wei, Z. Lu and J. Yu, *Sol. Energ. Mater. Sol. C.*, 2012, **105**, 220-228.
34. N. Lim, N. Cho, S. Paek, C. Kim, J. K. Lee and J. Ko, *Chem. Mater.*, 2014, **26**, 2283-2288.
35. M. C. Scharber, D. Mühlbacher, M. Koppe, P. Denk, C. Waldauf, A. J. Heeger and C. J. Brabec, *Adv. Mater.*, 2006, **18**, 789-794.
36. D. Bagnis, L. Beverina, H. Huang, F. Silvestri, Y. Yao, H. Yan, G. A. Pagani, T. J. Marks and A. Facchetti, *J. Am. Chem. Soc.*, 2010, **132**, 4074-4075.

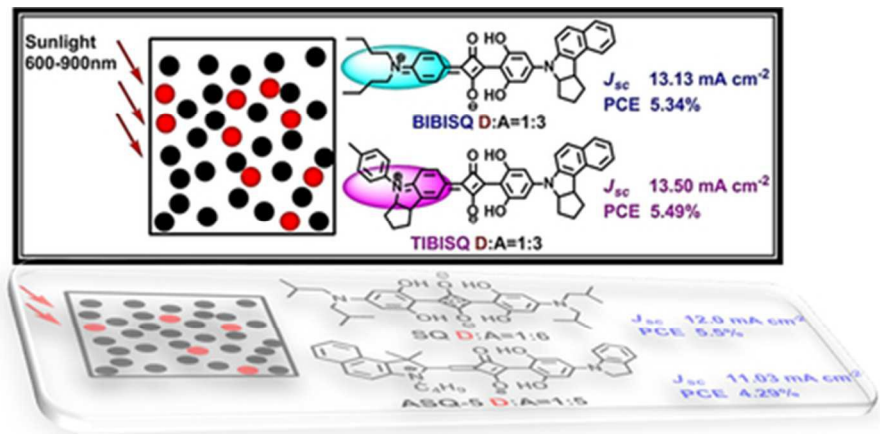
37. X. Guo, M. Zhang, J. Tan, S. Zhang, L. Huo, W. Hu, Y. Li and J. Hou, *Adv. Mater.*, 2012, **24**, 6536-6541.

[View Article Online](#)

DOI: 10.1039/C5RA24186C

Two unsymmetrical squaraines were employed as donors for high performance

BHJ-OPVs with $J_{sc} > 13 \text{ mA cm}^{-2}$ and PCE > 5%.



38x18mm (300 x 300 DPI)